Magnetic Resonance-Compatible Arm-Crank Ergometry: A New Platform Linking Whole-Body Calorimetry to Upper-Extremity Biomechanics and Arm Muscle Metabolism

Riemer JK Vegter (r.j.k.vegter@umcg.nl)
Rijksuniversiteit Groningen https://orcid.org/0000-0002-4294-6086
Sebastiaan van den Brink
Universitair Medisch Centrum Groningen
Leonora J Mouton
Universitair Medisch Centrum Groningen
Anita Sibeijn-Kuiper
Universitair Medisch Centrum Groningen
Lucas H.V. van der Woude
Universitair Medisch Centrum Groningen
Jeroen A.L. Jeneson
Universitair Medisch Centrum Groningen

Methodology

Keywords: Upper-extremity exercise, asynchronous arm-cranking, dynamometry, ergometry, muscle, oxidative metabolism, pH, EMG, indirect calorimetry, in vivo 31P Magnetic Resonance Spectroscopy

Posted Date: July 7th, 2020

DOI: https://doi.org/10.21203/rs.3.rs-37885/v1

Version of Record: A version of this preprint was published at Frontiers in Physiology on February 19th, 2021. See the published version at https://doi.org/10.3389/fphys.2021.599514.

Abstract

Background: Evaluation of the effect of human upper body training regimens may benefit from knowledge of local energy expenditure in arm muscles. To that end, we developed a novel asynchronous arm-crank ergometry platform for use in a clinical magnetic resonance (MR) scanner with ^{31}P spectroscopy capability to study arm muscle energetics. The utility of the platform was tested in an investigation of the impact of daily practice on the energetic efficiency of execution of an arm-cranking task (ACT) in healthy subjects.

Results: We recorded the first ever in vivo ^{31}P MR spectra from the human *biceps bracii* muscle during ACT execution pre- and post-three weeks of daily practice bouts, respectively. Complementary datasets on whole body oxygen consumption, arm muscle electrical activity, arm-force and power output, respectively, were obtained in the mock-up scanner. The mean gross mechanical efficiency of execution of the ACT significantly increased 1.5-fold from 5.7 ± 1.2% to 8.6 ± 1.7% ($P<0.05$) after training, respectively. However, in only one subject this improvement was associated with recruitment of strictly oxidative motor units in the working biceps muscle. In all other subjects, biceps pH fell below 6.8 during exercise indicating recruitment of anaerobic motor units, the magnitude of which was either unaffected (two subjects) or even increased (two subjects) post-training. Surface electromyography and mechanical force recordings revealed that individuals employed various arm muscle recruitment strategies, using either predominantly elbow flexor muscles (two subjects), elbow extensor muscles (one subject,) or a combination of the two (two subjects), respectively. Three weeks of training improved muscle coordination but did not alter individual strategies.

Conclusions: The new platform has produced the first ever in vivo dynamic data on human biceps energy and pH balance during upper body exercise. It allows evaluation of cyclic motor performance and outcomes of upper-body training regimens in healthy novices by integrating these new measurements with whole body calorimetry, surface electromyography and biomechanical measurements. This methodology may be equally valid for lower-limb impaired athletes, wheelchair users and patients with debilitating muscle disease.

Background

Optimal upper-extremity functioning is a prerequisite for healthy performance under different conditions, such as activities of daily living of persons with lower limb impairments, the work of many industrial labourers, or during different athletic disciplines. Upper-extremity cyclic exercise is indeed more straining and less efficient than leg exercise, while shoulders and wrists are prone to overuse complaints and pain (1). Whole body measures of exercise capacity and physical stress monitor the activation of a multitude of diverse and small muscle masses in a considerably more complex functional anatomy (2). Compared to lower-body exercise, upper body exercise roughly follows similar physiological and biomechanical pathways in exercise testing, training, practice and motor skill learning (3,4). Yet, absolute and relative

outcomes of cardiometabolic stress and efficiency are different between upper and lower body physical activity.

Whole-body measures of exercise physiology in upper body exercise (e.g., (5,6)) are limited in their detail in both healthy and clinical populations. Intramuscular metabolic processes during dynamic exercise require different, more local and preferably non-invasive measures to more accurately monitor and understand the energetic processes of exercise, adaptation, practice or training in healthy as well as clinical and pathologic populations (7). This will help render a more fundamental understanding of physiological and biomechanical mechanisms of function, adaptation and training, as well as pathology.

Here, we report on a novel experimental platform for investigation of upper-extremity cyclic exercise enabling in vivo biochemical and physiological data gathering from individual arm muscles as well as ensembles of arm muscles all the way up to the whole body. An existing MR-compatible leg-crank ergometer (8) was hereto adapted for asynchronous arm-crank ergometry (9–11) and implemented on a multi-nuclear MRI scanner for dynamic in vivo ^{31}P spectroscopic assay of ATP metabolism in human arm muscle. Complementary datasets on whole body oxygen consumption, upper extremity muscle electrical activity, force and power output during arm-crank exercise, respectively, were obtained in parallel experiments in a mock-up MRI scanner. The utility of the new platform was tested in a low-intensity arm-cycling practice experiment in five healthy individuals. Specifically, we tested the hypothesis that low-intensity practice in naïve test-subjects would result in motor skill learning causing improvements in upper-extremity muscle coordination as well as a reduction in oxidative energy requirement, respectively, during execution of a standardized arm-cranking task (ACT).

Methods

Table 1
Characteristics of the participants.

	PP 1	PP 2	PP 3	PP 4	PP 5
Age (year)	21	23	26	23	23
Length (m)	1.73	1.67	1.69	1.67	1.76
Weight (kg)	66	63	52	70	69
Arm span (m)	1.76	1.65	1.69	1.67	1.75
Gender	Male	Female	Male	Female	Male
PP – Participant.					

Participants

Five able-bodied naive participants were included in the study (Table 1). Only participants with a height of less than 1.80 m and a small to moderately broad upper body were included to enable arm-cycling inside

the 60-cm diameter bore of the MRI scanner that was used in the study. Other exclusion criteria were claustrophobia, hypersensitivity to loud noises or presence of metal inside the body. Lastly, individuals with prior arm-cycling experience were also excluded as the effect of practice is expected to be the highest at the beginning (12). It was ensured that the participants had no shoulder impairments or other injuries which could limit them in their ability to perform the cyclic exercise. All participants signed informed consent and passed the PAR-Q physical readiness questionnaire before the start of the study (13). The study was approved by the Local Ethics Committee, of the Centre for Human Movement Sciences, University Medical Centre Groningen, University of Groningen, the Netherlands.

Experimental design of low-intensity practice intervention.

The practice intervention in this study consisted of two pre-test trials, eight training sessions and two post-test trials resulting in a total of 80 minutes of active practice over a period of three weeks (Fig. 1). For each exercise bout, subjects were positioned supine and head-first on the bed of the (mock) MRI scanner and fitted with the carbon poles (Figs. 2 and 3). The elbow angle in starting position was 90 degrees in accordance with a maximum torque-angle relationship for the biceps muscle (14). Subjects were instructed to perform asynchronous arm-cycling exercise at 90 rounds per minute (rpm) guided by a metronome. A brake weight of 0.2 kg was applied to the flywheel yielding a workload of 15W at this crank rate (Supplemental Materials, Fig. 1). Pre- and post-test trial#1 as well as all training sessions were performed inside a mock-up version of the Achieva Intera MRI scanner (Fig. 3) to obtain data on (i) gas exchange, (ii) heart rate, (iii) force production, (iv) acceleration of the pole and (v) upper arm muscle activity, respectively, during execution of the asynchronous arm-cranking task (ACT). Pre- and post-test trial #2 was conducted inside a multi-nuclear 3T Achieva Intera MRI scanner to gather complementary data on biceps ATP turnover and pH dynamics during ACT execution.

MR-compatible arm-crank ergometer.

A previously described MR-compatible leg-crank cycle ergometer constructed from nonferrous materials to minimize interference with the static 3 T magnetic field of the MRI scanner (8) was refitted for arm-cranking. Two length-adjustable carbon ski poles (Leki, Italy) were hereto fitted with custom-made 3D printed carbon handles and attached to the ergometer cranks using ball joints custom-made from non-ferrous materials (Fig. 2). An additional pole was constructed and instrumented with a unidimensional forcesensor (LCM300 load cell; Futek, Irvine, CA, USA), and a MT-9 accelerometer (Xsens, Enschede, The Netherlands), respectively, for measurements of push/pull force output and acceleration of the right arm in a parallel series of experiments conducted in a mock-up MRI scanner (Fig. 3). The calibrated load cell and the accelerometer were both connected to the Porti 5 system (TMS International, Enschede, The Netherlands). The Porti 5 system measured forces and acceleration in millivolt (mV) with a sample frequency of 1600 Hz, yielding data of both pushing and pulling forces and the acceleration in X, Y and Z direction. Study subjects were additionally fitted with surface electrodes to the *m. Biceps* (*Longus &*

Brevis), *m. Brachioradialis*, *m. Triceps* (*Longus & Lateralis*), respectively, as well as a mask for spirometry (COSMED K4, Italy) enabling dynamic recording of surface EMG and breath-by-breath VO_2 and VCO_2 data, respectively, during asynchronous arm-cycling (Fig. 3).

Breath-by-breath spirometry

During pre-test 1 and post-test 1 gas exchange and heart rate were measured using breath-by-breath spirometry. The mobile Spirometer Cosmed K4B2 (COSMED, Italy) was used to analyse gas exchange during a 10-minute rest period prior to the trial, the 4-minute trial and a 10-minute long recovery period. Using VO_2 (L/min), VCO_2 (L/min) the internal energy expenditure was calculated (15). Subsequently, gross mechanical efficiency (ME) was determined using the calculated time-weighted average of internal energy expenditure over the final minute and the known workload of the arm-cycle. Calculations of the weighted average of heart rate and ME, respectively, were performed using custom written Matlab scripts (Matlab R2017a, The Mathworks, Natick, MA, USA) (16).

Concomitant with the spirometer, heartrate was collected through the same software and an additional heartrate strap provided by the same supplier. Delta heartrate is reported as the difference between resting heartrate before exercise and the heartrate during the steady-state phase of exercise (average of the final minute).

Force-sensor data processing

The raw push-pull output of the LCM300 load cell was processed using custom-written Matlab code. The force-sensor output was filtered using a fourth-order low-pass Butterworth filter at a cut-off frequency of 6 Hz to remove movement noise. The Porti 5 system measured the unidirectional (pushing & pulling) forces into the pole in mV and were transformed to N based on a calibration beforehand with known masses. Load cell output during the trial was consequently corrected for the output on the force-sensor during the 10 seconds in the static starting position prior to the trial. A typical example of the measured and corrected force output is shown in Fig. 2D. The mean and standard deviation of the height and width of the positive and negative peaks in the force signal of the whole trial were calculated. These values were used to illustrate the average unilateral force signal through the pole onto the crank of arm-cycle. Cubic spline data interpolation was used to create a smoothened pattern between the calculated average peak heights and widths. Due to technical difficulties with the Porti 5 system during force recording in subjects #2 and #4, these datasets were incomplete and are not reported.

sEMG activity data collection and processing

Surface EMG (sEMG) activity of the right arm of the participant was collected during pre-test 1 and post-test 1 using the Porti-5 system. The Porti-5 system measured EMG activity in mV at a sample frequency of 1600 Hz, PortiLab2 software was used for data acquisition. The skin of the participants was shaved, scrubbed and cleaned with alcohol to improve EMG electrode conductivity. As soon as the alcohol dried 2 EMG electrodes were patched upon the muscle belly of interest with approximately 0.02 m distance between the centre of the electrodes (Cleartrode, ConMed, USA). The following muscles were respectively

patched with electrodes and connected to the Porti system; Biceps Longus, Biceps Brevis, Triceps Longus, Triceps lateralis and Brachioradialis. Subsequently the participants were asked to take place in the starting position of the handcycle trial. Six Maximum Voluntary Contractions (MVCs) were performed on the handgrip equipped with the LCM300 load cell. The MVCs lasted 5 seconds and the participants had 2 minutes of rest between each MVC. Three flexion MVCs were performed followed by 3 extension MVC's. The MVC's were performed while keeping the flywheel and handcycle platform fixed to avoid movement of the arm-cycle handle relative to the participant.

The raw acquired output of the EMG activity was processed using custom written scripts in Matlab. EMG signals were filtered using a fourth order dual pass Butterworth filter setting. A high pass filter with a cut-off frequency of 6 Hz was performed on the raw EMG signal to remove low frequency noise. Subsequently, full wave rectification was performed by taking the absolute value of the signals. The rectified signal was low-pass filtered using a cut-off frequency of 10 Hz to create the linear envelope of the EMG signal. Using the EMG signals during the performed MVC's the relative percentage of EMG used during the trial was determined. Mean EMG signals of 0.5 seconds around the time point at which the force on the load cell reached its peak were calculated (0.125 s before the peak till 0.375 s after the peak). The three flexion MVC's were used to determine the maximum EMG signal of the Biceps Longus, Biceps Brevis and Brachioradialis. Accordingly, the three extension MVC's were used to determine the maximum EMG signal of the Triceps Longus and Triceps Lateralis. Subsequently EMG activity during the trial could be expressed as a percentage of the maximum EMG activity.

In vivo ^{31}P-MRS data collection and post-processing.

In vivo ^{31}P-MRS measurements were performed during pre-test 2 and post-test 2 in a 3 T Achieva Intera whole-body scanner (60 cm bore diameter; Philips Healthcare, the Netherlands). The arm-crank ergometer was bolted onto the scanner patient support. Subjects were positioned in supine, head-first position on the patient support (Fig. 1). A 6 cm diameter, single-turn send-receive ^{31}P surface coil (P60; Philips Healthcare, Best, the Netherlands) was positioned over the *m. Biceps Brevis* of the right arm of the study subjects. The coil was manually tuned and matched at the Larmor frequency of phosphorus-31 at 3 T (51.73 MHz). Free induction decays (FIDs) were next acquired using a 90-degree adiabatic excitation pulse. Firstly, a measurement of the basal phosphorus metabolite levels in the biceps muscle was performed (16 averaged FIDs; 2048 points, sample freq 3000 Hz; repetition time (TR) 13333 ms). During exercise, continuous spectroscopic data gathering was synchronized with arm-cranking frequency as described elsewhere (17). Here, FIDs were recorded with a repetition time of TR 2666 ms (corresponding to 4 rotations of the handcycle at 90 rpm). Four FIDs were averaged per individual spectrum and stored for off-line analysis.

FIDs were analysed in the time domain with respect to resonance amplitudes and frequencies of ATP, inorganic phosphate (Pi), phosphocreatine (PCr) and phosphomonoesters (PME) and quantified using the AMARES (Advanced Method for Accurate, Robust, and Efficient Spectral fitting) algorithm in the jMRUI

software package (version 3.0) using prior knowledge of starting values, line width, frequency and shape of the resonance peaks (18).

Intramuscular pH was calculated from the difference in resonance frequency between Pi and PCr (in parts per million (ppm)) as described elsewhere (19,20). For each subject, residual biceps PCr content (% of resting) and intramuscular pH in the final minute of ACT execution were determined as physiological endpoints.

Statistics

IBM SPSS Statistics version 25 was used for statistic calculations to determine changes over the practice intervention in the measured parameters a non-parametric Wilcoxon signed rank test for two related samples was used given the small sample size. A one-sided test was performed since only improvements in function were expected as a result of motor learning.

Results

Table 2
Changes in EMG, ME, HR and metabolic data for all participants pre-test versus post-test

	EMG ± SD (%)		**ME (%)**		**ΔHR**		**PCr (%)**		**pH**	
	pre	**post**	**pre**	**post**	**pre**	**post**	**pre**	**post**	**pre**	**post**
PP1	12.9 ± 7.6	9.6 ± 2.3	5.6	8.6	18	13	4.8	9.9	-0.76	-0.53
PP2	11.4 ± 3.7	12.6 ± 6.1	5.0	8.3	25	17	8	6.6	-0.18	-0.19
PP3	11.5 ± 9.0	7.1 ± 3.3	6.1	6	26	22	11.1	61.6	-0.45	-0.13
PP4	26.2 ± 9.2	11.0 ± 2.1	4.3	10.7	60	24	12.4	7	-0.11	-0.36
PP5	4.9 ± 1.5	3.8 ± 1.9	7.6	9.3	17	12	60.9	57.9	-0.09	-0.28
Mean ± SD	**13.4 ± 7.8**	**8.8 ± 3.5**	**5.7 ± 1.2**	**8.6 ± 1.7**	**29.0 ± 17.5**	**17.4 ± 5.1**	**19.4 ± 23.4**	**28.6 ± 28.5**	**-0.32 ± 0.29**	**-0.30 ± 0.16**
p value	0.069		0.04*		0.021*		0.446		0.446	

EMG – Electromyography; ME – Mechanical Efficiency; EE – Energy Expenditure; ΔHR – Delta Heart Rate; PCr – Phosphocreatine; PME – Phosphomonoester.

Practice intervention - group results.

All five participants completed the arm-cycling practice intervention. An overview of the pooled findings with respect to pre- versus post-training EMG activity, ME, HR, biceps energy balance and pH balance during exercise are presented in Table 2. The training intervention resulted in a significant increase of mechanical efficiency of execution of the four-minute arm-cycling task (5.7 ± 1.2 versus 8.6 ± 1.7, pre-training versus post-training; P = 0.04) concomitant with a reduction in delta HR over time (29.0 ± 17.5 bpm versus 17.4 ± 5.1 bpm, p = 0.02). No significant change in total scaled EMG activity was found between pre- and post-training execution of the arm-cycling task (13.4 ± 7.8 versus 8.8 ± 3.5, p = 0.07). Likewise, no significant mean improvement of biceps energy and pH balance during execution of the arm-cycling task was found for the group when comparing pre- versus post-training.

Practice intervention – effect on ME and biceps acidification in individuals

Figure 4 shows the individual outcomes for *in vivo* biceps pH measured in the final minute of ACT execution (left panel) compared to gross ME of ACT execution calculated on basis of whole-body IC measurements (right panel). In four study subjects, the practice intervention resulted in an improvement of gross ME of ACT execution (subjects (#1, #2, #4 and #5). In subject #3, ME did not improve in response to the training. Changes to the magnitude of biceps muscle acidification during ACT execution in response to the practice intervention were more variable. Specifically, in subjects #1 and #3, biceps acidification during ACT execution post-training was 0.2–0.3 pH units less than pre-training, whereas in subjects #4 and #5 the reverse was found (Fig. 4). In subject #2, biceps acidification during ACT was unaffected by the practice intervention.

Practice intervention – effect on arm muscle activity in individuals

Our pre-test sEMG recordings during ACT execution revealed that individual subjects employed distinctly different upper arm muscle recruitment strategies to generate sufficient power output to perform the task (Fig. 5, left column). Specifically, participants either predominantly used upper arm flexor muscles including the *m. biceps brevis* (participant 1 and 2), upper arm extensor muscles (*m. triceps longus* and *lateralis*, respectively; participant 3) or a combination of both (participant 4, and 5), respectively. When comparing to post-training EMG recordings, training did not result in any major change in individual muscle recruitment strategy during handcycling except for subject #1 (Fig. 5, right column). In subjects #1, #3 and #4, the training intervention resulted in lower amplitudes of EMG recordings from their dominantly recruited upper arm muscles (flexor, extensor and mix, respectively; Fig. 3, right column), whereas no such change in EMG amplitude as a result of training was observed in subjects #2 and #5 (Fig. 5, right column).

Practice intervention – effect on arm force output in individuals

Figure 6 shows the average dynamics of mechanical force generation during execution of the handcycling task prior to the training intervention (left column) versus post-training (right column) for subjects #1, #3 and #5 (2&4 miss because of measurement error). In each case, two complete cycles were averaged over the whole trial. In line with the EMG recordings shown above (Fig. 5), subject #1 mostly produced net positive forces during pre-training execution of the handcycling task indicating pulling (flexor) movements on the load cell, while subject #3 mostly produced net negative forces indicate pushing (extensor) movements (Fig. 6, left column). Subject #5 evenly alternated pulling and pushing during handcycling in the pre-test (Fig. 5, left column). The training intervention resulted in all three subjects in a much-improved reproducibility of mechanical force generation during handcycling as evidenced by a twofold or more reduction of variance (Fig. 6, right column). The force recordings in subject #5 suggest that the training intervention resulted in a slight shift from a mixed push-pull strategy towards a predominantly push strategy (Fig. 6).

Practice intervention – effect on biceps energy- and pH balance in individuals

Figure 7 shows time series of in vivo ^{31}P MRS spectra of the *biceps* muscle recorded during ACT execution in two individuals illustrating employment of a pull arm-cranking strategy predominantly involving the *biceps* muscle of the upper arm (left; subject #1, post-training) versus a push strategy involving predominantly the *triceps* muscle (right; subject #3, post-training), respectively. The difference in strategy between the two individuals was reflected in the extent of intramuscular Pi accumulation and complementary PCr depletion of the *biceps* during ACT execution in each subject post-training (Fig. 7). Specifically, PCr in fibres of the biceps muscle in subject #1,was almost completely depleted and the resonance frequency and linewidth of the Pi signal evidenced severe muscle acidification (pH 6.5 versus 7.1 in resting biceps) (Fig. 7, left stack). In contrast, PCr depletion, Pi accumulation and acidification of muscle fibres in the *biceps* muscle of subject #3 during execution of the standard handcycling task were all minor (Fig. 7, right stack). The presence of additional significant signal upfield from the broad Pi resonance in the in vivo ^{31}P MR spectrum acquired in the final minute of handcycling in subject #1 (Fig. 7, left stack) was attributed to accumulation of hexose monophosphates (HMP) in anaerobic fast-twitch glycolytic fibers.

Discussion

The primary innovation of the presented experimental platform for investigation of upper-extremity cycling exercise in humans is that it enables dynamic, quantitative in vivo assay of ATP metabolism and pH balance in working muscles of the upper arm in addition to conventional physiological measures such as whole-body oxygen consumption. Thus, it can uniquely inform on contributions of oxidative versus anaerobic ATP production of individual muscles of the upper arm during execution of any particular arm-cranking task. Below, we will discuss how this new information impacted the outcome of the practice intervention study in healthy naïve subjects showcasing the platform, as well as technological and practical aspects of the platform including recommendations for future upgrading and use.

Outcome of the practice intervention study.

The practice intervention study that we conducted to showcase the new platform tested the hypothesis that three weeks of daily training would improve the gross mechanical efficiency of execution of a physical task consisting of supine asynchronous arm-cranking at 90 rpm for 6 min against a workload of 15W. Tested solely against the combined results of the conventional physiological measures that we collected, this hypothesis was not rejected: the mean gross ME of ACT execution significantly improved after training in the study test-population (Table 2). The in vivo ^{31}P MRS recordings from biceps muscle during ACT execution that we additionally collected, however, showed that, with respect to this particular physiological measure, this outcome was biased by results in subjects #4 and #5. Specifically, these two individuals had recruited more fast-twitch fibers with low oxidative capacity (FG fibers; (21)) to perform the ACT trial post-training than pre-training, as evidenced by increased biceps muscle acidification (Fig. 4). Neither of these subjects had appreciably changed their arm-cranking strategy towards any 'pull' mechanism in response to practice; if any, subject #5 had rather adopted more of a 'push' strategy (Fig. 6). Therefore, the outcome of the ratio of whole arm power-output and whole-body energy expenditure during ACT execution was skewed towards a higher ratio post-training (Table 2). This particular finding was similar to results of a recent study of the effect of a low-intensity training intervention in manual wheelchair propulsion in naïve subjects (22). Specifically, the authors reported improvement of gross ME of wheelchair propulsion concomitant with opposite rather than parallel changes in power-output over time for the *biceps* and *brachialis* muscles of the upper arm. Notably, power-output of the *biceps* muscle was found to increase, not decrease with training (22) Together, these studies indicate that findings of increased ME after training of any form of upper body exercise based solely on whole body measurements of oxygen consumption should be interpreted with caution. The new experimental platform for upper-extremity cyclic exercise presented in this report uniquely affords to gather complementary data on energy expenditure in upper-extremity muscles to strengthen objective evaluation of the outcome of upper body training interventions.

The results of the practice intervention study also provide new insight into the contribution of aerobic versus anaerobic ATP metabolism in muscles recruited during cyclic upper-body exercise. As discussed in the above, the data showed that the assumption of strictly aerobic muscular ATP metabolism at low-intensity dynamic upper-body exercise implicit in the use of the parameter 'gross ME' to evaluate training outcome (23,24) did not hold for the majority of untrained, able-bodied, healthy individuals that participated in the present study. Secondly, we found that the contribution of anaerobic motor units of the biceps to power-output during arm-cycling was not uniformly affected by the training intervention across test subjects. Inter-individual differences in learning efficacy have previously been described (7,25–29) and may become more explicitly characterized using this platform.

The novelty of the current approach comes with some technological limitations that should be considered when assessing the results. First, subjects performed the ACT trial twice – i.e., inside the mock-up MRI scanner and inside the MRI scanner, respectively – both pre- as well as post-training in order to obtain a complete set of experimental data consisting of sEMG, mechanical force and PO, spirometry

and ^{31}P MRS recordings, respectively (Fig. 1). As such, it was assumed that individual participants performed the physical task in both environments in identical manner. Past findings that motor skill acquisition takes place on a timescale of multiple minutes (25) suggests that this assumption may perhaps have been problematic. However, our results showed that individual arm-cycling strategies were consistent over the entire course of the experiment and did not majorly change during training. Secondly, our practice intervention study employing the new platform was limited in its sample-size resulting in low statistical power of evaluation of the study outcome for the group. Here, both the high cost as well as limited availability of MRI scanner time played a role. However, the observed heterogeneity in individual ACT strategy within these five subjects in and by itself suggests that a common group pattern of task execution may perhaps not be expected. On the other hand, past evidence suggests that motor skill acquisition is a general principle of motor functioning and, as such, should hold for groups of subjects (23,30,31). Therefore, it should be of interest to study in a larger population of test subjects if the results of the present study can be reproduced.

Technological and practical aspects of the platform.

sEMG and force sensor recordings.

Upper-arm muscle recruitment patterns in participants performing cyclic upper-body exercise were well reflected by the results of both sEMG and force-sensor recordings during ACT execution (Figs. 5 and 6, respectively). Of these, sEMG is commonly available in movement research labs evaluating cyclic upper-body exercise (32–34). The force-sensor/pole ensemble was custom-built using an ‘off the shelf’ one-dimensional sensor incorporated in the pole, whereby the pole handles were constructed such that no torque was possible (Methods; Fig. 3). Although the force-sensor recordings lacked the detail on individual muscle contributions to overall arm power-output provided by sEMG (Fig. 5), the former adequately distinguished flexor from extensor movements with superior signal-to-noise and superior dimensionality (i.e., N; (Fig. 6). Moreover, while similar pictures on arm muscle recruitment during ACT execution in individual subjects emerged from the sEMG and force-sensor recordings in the present study, the latter suggested training induced a small shift from ‘mixed push/pull’ to ‘pull’ mode in subject #5 that was less evident from the sEMG recordings.

In vivo ^{31}P MRS.

The principal practical problem we had to overcome to robustly collect ^{31}P MRS data from the human biceps muscle during high-frequency arm-cycling with ~ 10 s time resolution and adequate signal-to-noise and resonance linewidth quality for quantitative analysis, was the anatomy of human subjects in relation to MRI scanners. Specifically, the biceps muscle is physically on the periphery of the human body, typically some 25 cm out of the central body axis in lean adults, whereas the default ‘sweet spot’ of static field magnetic homogeneity of 3 T MRI scanners is typically a 20–30 cm diameter sphere in the center of the magnet. In addition, the inner-diameter of the bore of commonly available clinical MRI scanners including the MRI scanner used in the present study, is 60 cm. Together, this both limited the attainable

quality of local static magnetic field homogeneity ('shim') over the biceps muscle (typical PCr linewidth 30–40 Hz compared to 5–10 Hz in in vivo ^{31}P MR spectra of medial quadriceps of the upper leg (35) as well as constrained the physical space for arm exercise inside the magnet. Any additional signal quality deterioration introduced by motion artefacts during high-frequency arm-cycling (i.e., 90 rpm) was surprisingly minor. We attributed this to the fact that the upper arm remains in one and the same position during arm-cycling around the elbow (Fig. 2). In addition, ^{31}P MRS data acquisition from the biceps during exercise was synchronized with cycling phase using a custom-built triggering setup described elsewhere (8). Together, this enabled robust dynamic ^{31}P MRS data gathering from the biceps muscle during high-frequency arm cycling with 11 s time resolution in all subjects (Fig. 7).

Recommendations for future platform upgrading and use.

All sEMG, spirometry and mechanical force data recordings were conducted in a parallel series of pre- and post-training tests in a mock-MRI scanner due to issues of MR-compatibility of equipment. Ideally, all these recordings should be done concomitantly with the MR measurements. This should, in fact, be feasible. MR-compatible approaches to collect VO_2 and VCO_2 data are available including Douglas bag-based methodologies (36–38) or mass-spectrometry(39). Likewise, simultaneous acquisition of sEMG and ^{31}P MRS data, respectively, from the upper arm muscles are well feasible provided non-gradient-based data acquisition sequences are employed such as used in the present study(40). Similarly, the applied torque over the cycle of the crank of the MRI-compatible handcycle ergometer should ideally also be measured in the MRI scanner. While such systems are available and have been used for arm-cranking and hand-cycling studies (12,33,41), these are as of yet MRI-incompatible. The sole available industry-standard MRI cycle ergometer (Lode BV, Groningen, the Netherlands) could potentially be fitted with hardware and software to render such measurements feasible in MRI scanners in the future (Jan-Reinder Franssen, Lode BV, personal communication).

In vivo ^{31}P MR spectra were collected from the biceps muscle using a single element ^{31}P surface coil that was available in our laboratory. In light of our findings of inter-individual differences in pull- versus push-handcycling strategies, spectra should also be collected from the triceps muscle, preferably simultaneously from both muscles. In principle, use of a two-element ^{31}P surface coil in combination with dual receive channels should render simultaneous collection of in vivo ^{31}P MR spectra from both upper arm muscles feasible. Modern clinical 3T MRI scanners with multinuclear capability from major vendors typically readily support use of such advanced coil designs. Moreover, these scanners are typically also available in a 70-cm diameter bore size. This both greatly enhances room for in-magnet exercise as well as relaxes some of the constraint on physical dimensions of study subjects that we encountered.

Lastly, the new platform for upper-extremity cycling exercise presented here may be useful for clinical investigations of a range of study populations and objectives. Firstly, it may contribute to guide training of athletes relying on upper-body activities including rowing, arm-cycling, sailing, rock-climbing or wheelchair track athletes. In these sports the upper-body is highly trained, yet little remains known about fibre-type distributions and relative contributions of aerobic and anaerobic energy production optimal for

each particular athletic activity, for upper- and lower-extremities alike (42). Secondly, the methodology may also be useful in the field of rehabilitation of individuals with spinal cord injury. These often-traumatic injuries render individuals heavily dependent on their upper-body for daily activity, while there may be a large heterogeneity in upper-body fitness and skill prior to the accident. Of specific interest are any adaptation processes taking place at muscular levels as well as to local and bodily physiology as a consequence of continuous practice and use of their upper body (43). Other potential clinical application of the methodology may be in care for patients with neuromuscular disease, primary metabolic myopathies including mitochondrial myopathies as well as secondary myopathies including heart failure and COPD. Here, the key asset is the fact that arm-cranking constitutes a relatively low intensity dynamic exercise paradigm (dynamic range 3–25 W at 90 rpm; Supplemental Materials, Fig. 1) compared to conventional testing using bicycle ergometers. As such, it offers a platform to evaluate the quality of their muscles with respect to mechanical and metabolic functions and monitor the effects of training, pharmaceutical and dietary therapy.

Conclusion

The newly developed platform has produced the first ever in vivo data on human biceps energy- and pH balance during dynamic exercise in the context of biomechanical and system physiological outcomes. Integration of these measurements with whole body calorimetry, surface electromyography and mechanical measurements during arm-cycling training intervention showed that the study outcome of improved mechanical efficiency post-training was biased by variable contributions of anaerobic motor units of the biceps to power-output during arm-cycling among these novice subjects. This methodology may aid design and evaluation of upper-body training regimens for athletes, wheelchair-bound individuals and patients with debilitating muscle disease.

Declarations

Ethics approval and consent to participate

The study was approved by the Local Ethics Committee, of the Centre for Human Movement Sciences, University Medical Centre Groningen, University of Groningen, the Netherlands.

Consent for publication

All participants signed informed consent

Availability of data and materials

The datasets used and/or analysed during the current study are available from the corresponding author on reasonable request.

Competing interests

The authors declare that they have no competing interests

Funding

Not applicable

Authors' contributions

RV contributed to the conception and design of the work; the acquisition, analysis, and interpretation of data; and drafted the work. RV approves the submitted version (and any substantially modified version that involves the author's contribution to the study); RV has agreed both to be personally accountable for the author's own contributions and to ensure that questions related to the accuracy or integrity of any part of the work, even ones in which the author was not personally involved, are appropriately investigated, resolved, and the resolution documented in the literature.

SB contributed to the conception and design of the work; the acquisition, analysis, and interpretation of data; and drafted the work. SB approves the submitted version (and any substantially modified version that involves the author's contribution to the study); SB has agreed both to be personally accountable for the author's own contributions and to ensure that questions related to the accuracy or integrity of any part of the work, even ones in which the author was not personally involved, are appropriately investigated, resolved, and the resolution documented in the literature.

LM contributed to the conception and design of the work; interpretation of data; and drafted the work. LM approves the submitted version (and any substantially modified version that involves the author's contribution to the study); LM has agreed both to be personally accountable for the author's own contributions and to ensure that questions related to the accuracy or integrity of any part of the work, even ones in which the author was not personally involved, are appropriately investigated, resolved, and the resolution documented in the literature.

AS contributed to the design of the work; the acquisition, analysis, and interpretation of data. AS approves the submitted version (and any substantially modified version that involves the author's contribution to the study); AS has agreed both to be personally accountable for the author's own contributions and to ensure that questions related to the accuracy or integrity of any part of the work, even ones in which the author was not personally involved, are appropriately investigated, resolved, and the resolution documented in the literature.

LW contributed to the conception and design of the work; the acquisition, analysis, and interpretation of data; and drafted the work. LW approves the submitted version (and any substantially modified version that involves the author's contribution to the study); LW has agreed both to be personally accountable for

the author's own contributions and to ensure that questions related to the accuracy or integrity of any part of the work, even ones in which the author was not personally involved, are appropriately investigated, resolved, and the resolution documented in the literature.

JJ contributed to the conception and design of the work; the acquisition, analysis, and interpretation of data; and drafted the work. JJ approves the submitted version (and any substantially modified version that involves the author's contribution to the study); JJ has agreed both to be personally accountable for the author's own contributions and to ensure that questions related to the accuracy or integrity of any part of the work, even ones in which the author was not personally involved, are appropriately investigated, resolved, and the resolution documented in the literature

References

1. van der Woude LH, Veeger HE, Dallmeijer AJ, Janssen TW, Rozendaal LA. Biomechanics and physiology in active manual wheelchair propulsion. Med Eng Phys. 2002/01/22. 2001;23(10):713–33.
2. Veeger HE, van der Helm FC. Shoulder function: the perfect compromise between mobility and stability. J Biomech. 2007/01/16. 2007;40(10):2119–29.
3. Jones A, Poole D. Oxygen Uptake Kinetics in Sport, Exercise and Medicine. J Sports Sci Med. 2005 Mar 1;4(1):84.
4. Sparrow WA. Energetics of human activity. 2000.
5. Kraaijenbrink C, Vegter RJK, Hensen AHR, Wagner H, Van Der Woude LHV. Different cadences and resistances in submaximal synchronous handcycling in able-bodied men: Effects on efficiency and force application. PLoS One. 2017;12(8).
6. de Groot S, Vegter RJK, Vuijk C, van Dijk F, Plaggenmarsch C, Sloots M, et al. WHEEL-I: DEVELOPMENT OF A WHEELCHAIR PROPULSION LABORATORY FOR REHABILITATION. J Rehabil Med. 2014;
7. Vegter RJK, Lamoth CJ, de Groot S, Veeger D, van der Woude LH V. Inter-Individual Differences in the Initial 80 Minutes of Motor Learning of Handrim Wheelchair Propulsion. PLoS One. 2014;
8. Jeneson JAL, Schmitz JPJ, Hilbers PAJ, Nicolay K. An MR-compatible bicycle ergometer for in-magnet whole-body human exercise testing. Magn Reson Med. 2010;63(1):257–61.
9. van Drongelen S, Maas JC, Scheel-Sailer A, Van Der Woude LH. Submaximal arm crank ergometry: Effects of crank axis positioning on mechanical efficiency, physiological strain and perceived discomfort. J Med Eng Technol. 2009/02/12. 2009;33(2):151–7.
10. Dallmeijer AJ, Ottjes L, de Waardt E, van der Woude LH. A physiological comparison of synchronous and asynchronous hand cycling. Int J Sport Med. 2004/11/09. 2004;25(8):622–6.
11. Powers SK, Beadle RE, Mangum M. Exercise efficiency during arm ergometry: effects of speed and work rate. J Appl Physiol. 2017;56(2):495–9.

12. Kraaijenbrink C, Vegter RJK, Hensen AHR, Wagner H, Van Der Woude LHV. Biomechanical and physiological differences between synchronous and asynchronous low intensity handcycling during practice-based learning in able-bodied men. J Neuroeng Rehabil. 2020;
13. Thomas S, Reading J, Shephard RJ. Revision of the Physical Activity Readiness Questionnaire (PAR-Q). Can J Sport Sci. 1992;
14. Pinter IJ, Bobbert MF, van Soest AJK, Smeets JBJ. Isometric torque-angle relationships of the elbow flexors and extensors in the transverse plane. J Electromyogr Kinesiol. 2010;
15. Garby L, Astrup A. The relationship between the respiratory quotient and the energy equivalent of oxygen during simultaneous glucose and lipid oxidation and lipogenesis. Acta Physiol Scand. 1987;129.
16. Vegter R, Lamoth C, de Groot S, Veeger D, van der Woude L. Variability in bimanual wheelchair propulsion: consistency of two instrumented wheels during handrim wheelchair propulsion on a motor driven treadmill. J Neuroeng Rehabil. 2013;10(1):9.
17. van Brussel M, van Oorschot JWM, Schmitz JPJ, Nicolay K, van Royen-Kerkhof A, Takken T, et al. Muscle Metabolic Responses During Dynamic In-Magnet Exercise Testing: A Pilot Study in Children with an Idiopathic Inflammatory Myopathy. Acad Radiol. 2015;22(11):1443–8.
18. Vanhamme L, Van Den Boogaart A, Van Huffel S. Improved Method for Accurate and Efficient Quantification of MRS Data with Use of Prior Knowledge. J Magn Reson. 1997;
19. Prompers JJ, Jeneson JAL, Drost MR, Oomens CCW, Strijkers GJ, Nicolay K. Dynamics MRS and MRI of skeletal muscle function and biomechanics. NMR in Biomedicine. 2006.
20. Tobin RB, Mackerer CR, Mehlman MA. pH effects on oxidative phosphorylation of rat liver mitochondria. Am J Physiol Content. 1972 Jul 1;223(1):83–8.
21. Meyerspeer M, Boesch C, Cameron D, Dezortová M, Forbes SC, Heerschap A, et al. 31P magnetic resonance spectroscopy in skeletal muscle: Experts' consensus recommendations. NMR Biomed. 2020;
22. Vegter RJK, Hartog J, De Groot S, Lamoth CJ, Bekker MJ, Van Der Scheer JW, et al. Early motor learning changes in upper-limb dynamics and shoulder complex loading during handrim wheelchair propulsion. J Neuroeng Rehabil. 2015;
23. Almasbakk B, Whiting HT, Helgerud J. The efficient learner. Biol Cybern. 2001/02/24. 2001;84(2):75–83.
24. Garby L, Astrup A. The relationship between the respiratory quotient and the energy equivalent of oxygen during simultaneous glucose and lipid oxidation and lipogenesis. Acta Physiol Scand. 1987/03/01. 1987;129(3):443–4.
25. Vegter R, de Groot S, Lamoth C, Veeger D, Van der Woude L. Initial Skill Acquisition of Handrim Wheelchair Propulsion: A New Perspective. Neural Syst Rehabil Eng IEEE Trans. 2013;PP(99):1.
26. Kostrubiec V, Zanone pier-G, Fuchs A, Kelso JAS. Beyond the blank slate: routes to learning new coordination patterns depend on the intrinsic dynamics of the learner óexperimental evidence and theoretical model. Front Hum Neurosci. 2012;6:222.

27. Bouchard C, Rankinen T. Individual differences in response to regular physical activity. 2001. p. S446-51.
28. Withagen R, van Wermeskerken M. Individual differences in learning to perceive length by dynamic touch: evidence for variation in perceptual learning capacities. Atten Percept Psychophys. 2009/03/24. 2009;71(1):64–75.
29. King AC, Ranganathan R, Newell KM. Individual differences in the exploration of a redundant space-time motor task. Neurosci Lett. 2012;529(2):144–9.
30. Sparrow WA, Hughes KM, Russell AP, Le Rossignol PF. Movement economy, preferred modes, and pacing. In: Energetics of human activity. Champaign, IL, US: Human Kinetics; 2000. p. 96–123.
31. Lay BS, Sparrow WA, Hughes KM, O'Dwyer NJ. Practice effects on coordination and control, metabolic energy expenditure, and muscle activation. Hum Mov Sci. 2003/03/07. 2002;21(5–6):807–30.
32. Litzenberger S, Mally F, Sabo A. Influence of different seating and crank positions on muscular activity in elite handcycling - A case study. In: Procedia Engineering. 2015. p. 355–60.
33. Quittmann OJ, Meskemper J, Abel T, Albracht K, Foitschik T, Rojas-Vega S, et al. Kinematics and kinetics of handcycling propulsion at increasing workloads in able-bodied subjects. Sport Eng. 2018;21(4):283–94.
34. Abbasi Bafghi H, De Haan A, Horstman A, Van Der Woude L. Biophysical aspects of submaximal hand cycling. Int J Sports Med. 2008;29(8):630–8.
35. Schmitz JPJ, Van Riel NAW, Nicolay K, Hilbers PAJ, Jeneson JAL. Silencing of glycolysis in muscle: Experimental observation and numerical analysis: Experimental Physiology-Research Paper. Exp Physiol. 2010;95(2):380–97.
36. Voorhees A, An J, Berger KI, Goldring RM, Chen Q. Magnetic resonance imaging-based spirometry for regional assessment of pulmonary function. Magn Reson Med. 2005;
37. McLaughlin JE, King GA, Howley ET, Bassett DR, Ainsworth BE. Validation of the COSMED K4 b2 portable metabolic system. Int J Sports Med. 2001;
38. Rietjens GJWM, Kuipers H, Kester ADM, Keizer HA. Validation of a computerized metabolic measurement system (Oxycon-Pro®) during low and high intensity exercise. Int J Sports Med. 2001;
39. Whipp BJ, Rossiter HB, Ward SA, Avery D, Doyle VL, Howe FA, et al. Simultaneous determination of muscle and O2 uptake kinetics during whole body NMR spectroscopy. J Appl Physiol. 1999;
40. Vestergaard-Poulsen P, Thomsen C, Sinkjær T, Henriksen O. Simultaneous 31P NMR spectroscopy and EMG in exercising and recovering human skeletal muscle: Technical aspects. Magn Reson Med. 1994;
41. Vegter RJK, Mason BS, Sporrel B, Stone B, van der Woude LH V., Goosey-Tolfrey VL. Crank fore-aft position alters the distribution of work over the push and pull phase during synchronous recumbent handcycling of able-bodied participants. Sandbakk Ø, editor. PLoS One. 2019 Aug 19;14(8):e0220943.

42. Van Der Zwaard S, Van Der Laarse WJ, Weide G, Bloemers FW, Hofmijster MJ, Levels K, et al. Critical determinants of combined sprint and endurance performance: An integrative analysis from muscle fiber to the human body. FASEB J. 2018;
43. Van Der Scheer JW, Ginis KAM, DItor DS, Goosey-Tolfrey VL, Hicks AL, West CR, et al. Effects of exercise on fitness and health of adults with spinal cord injury: A systematic review. Neurology. 2017.

Figures

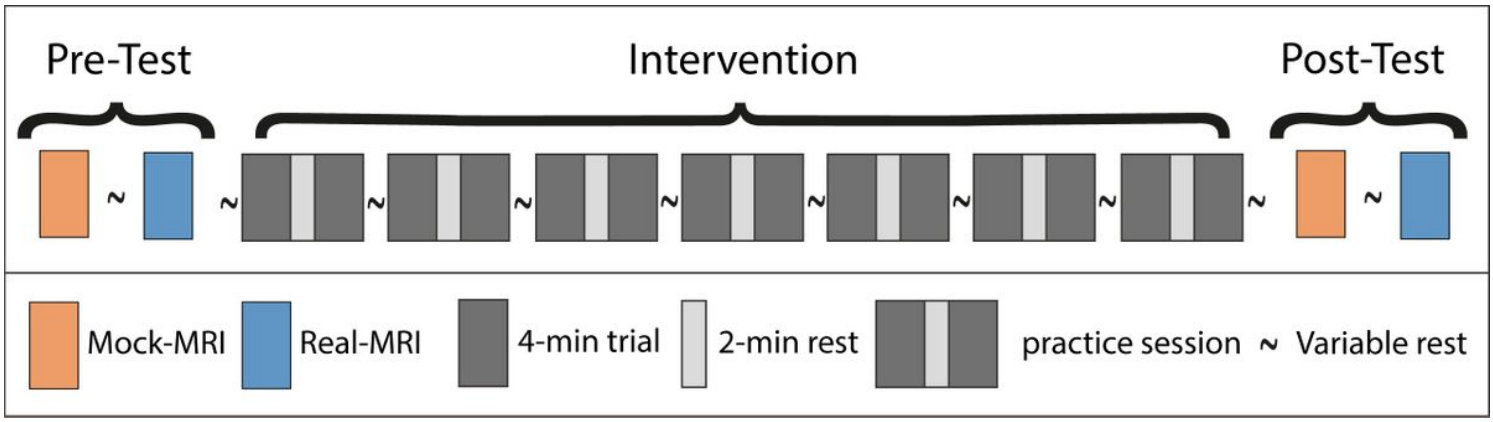

Figure 1

Experimental design of the low-intensity arm-crank practice intervention. Subjects performed a standard arm-cranking task (ACT; see Methods) prior to and following 3 weeks of daily practice (grey blocks). For the pre- and post-training tests, subjects performed two bouts of ACT: one inside a mock-up MRI scanner (orange blocks) and a second bout inside a MRI scanner (blue blocks), respectively, to facilitate acquisition of a comprehensive dataset including bodily oxygen consumption, upper arm muscle activity, force, in vivo ATP turnover and pH changes in biceps muscle.

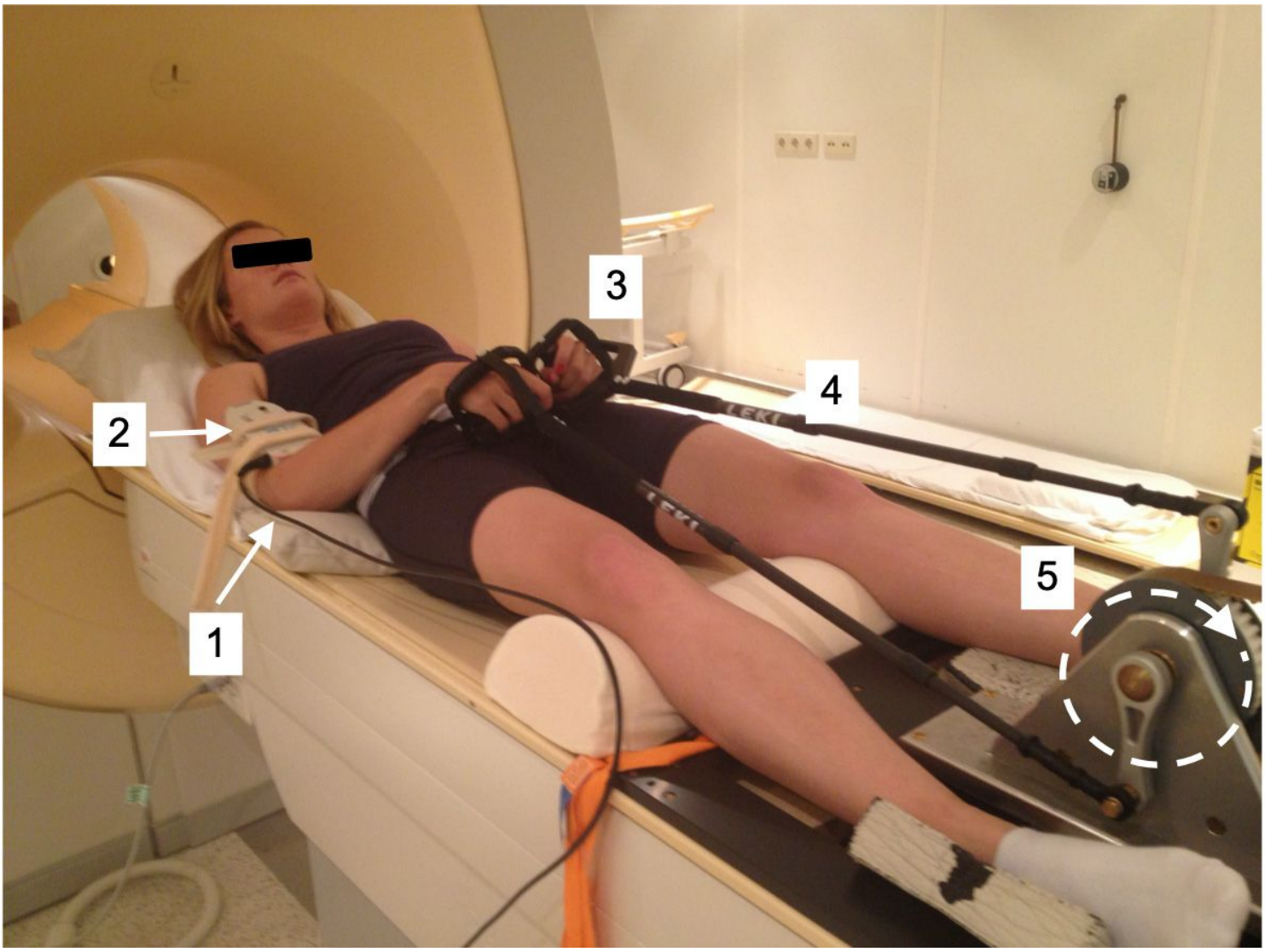

Figure 2

Test subject mounted supine, head-first on patient support of MRI scanner fitted with arm-crank ergometer. [1] stationary elbow joint; [2] 31P send-receive surface coil (Philips Healthcare); [3] carbon handgrips; [4] adjustable-length carbon ski poles (Leki, Italy); [5] rotating crank-wheel connected via a nylon belt to a wooden fly-wheel with mechanical brake.

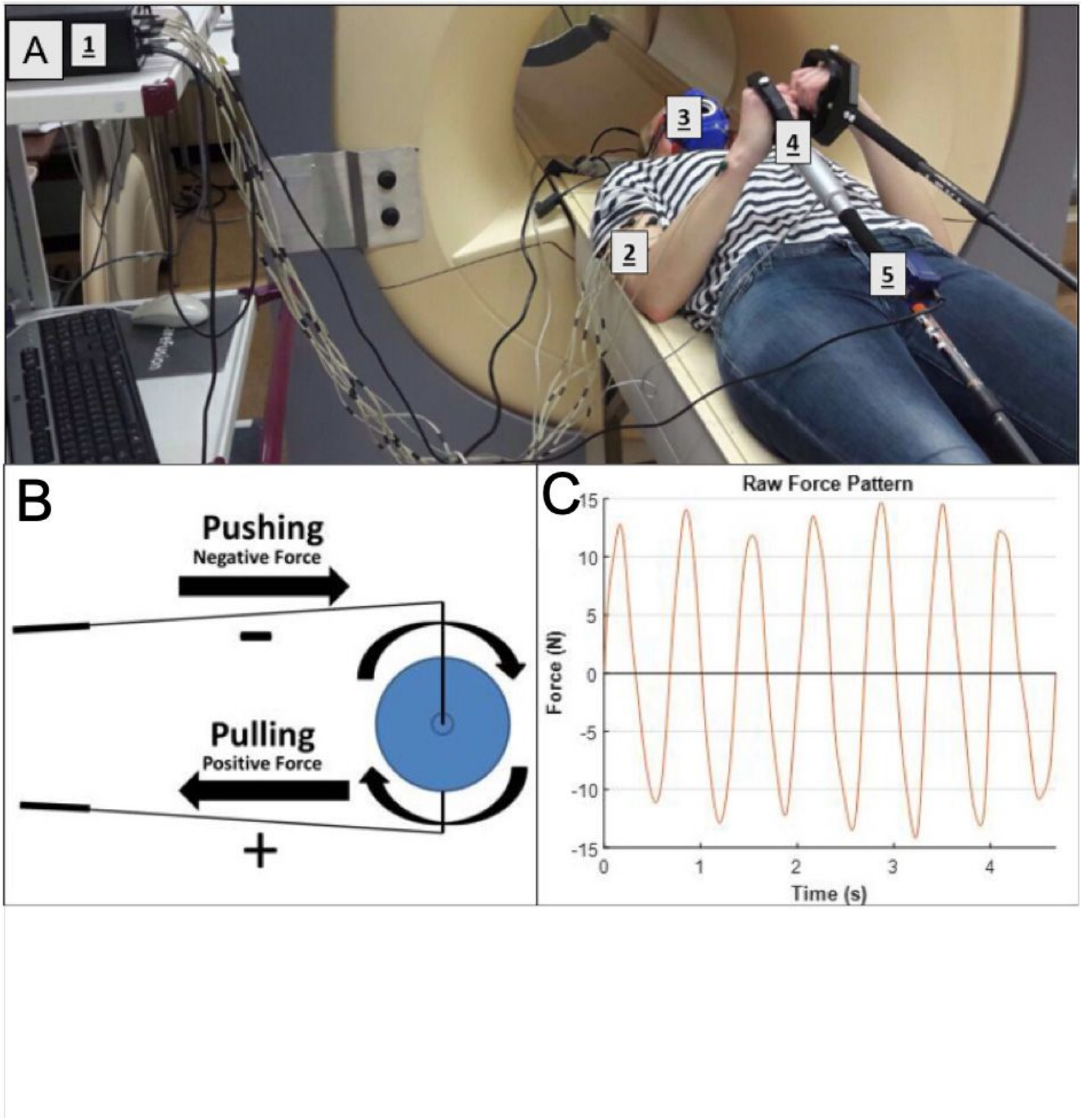

Figure 3

(A) test-subject mounted supine, head-first on patient support of mock-up MRI scanner fitted with arm-crank ergometer. [1] Porti 5 data recording & storage system; [2] EMG electrodes; [3] mask fro Breath-by-breath spirometry; [4] LCM300 load cell of instrumented pole; [5] MT-9 accelerometer attached onto pole. (B) Illustration of forces applied to the crank (C) excerpt from force recording on the LCM300 load cell during arm-cranking exercise.

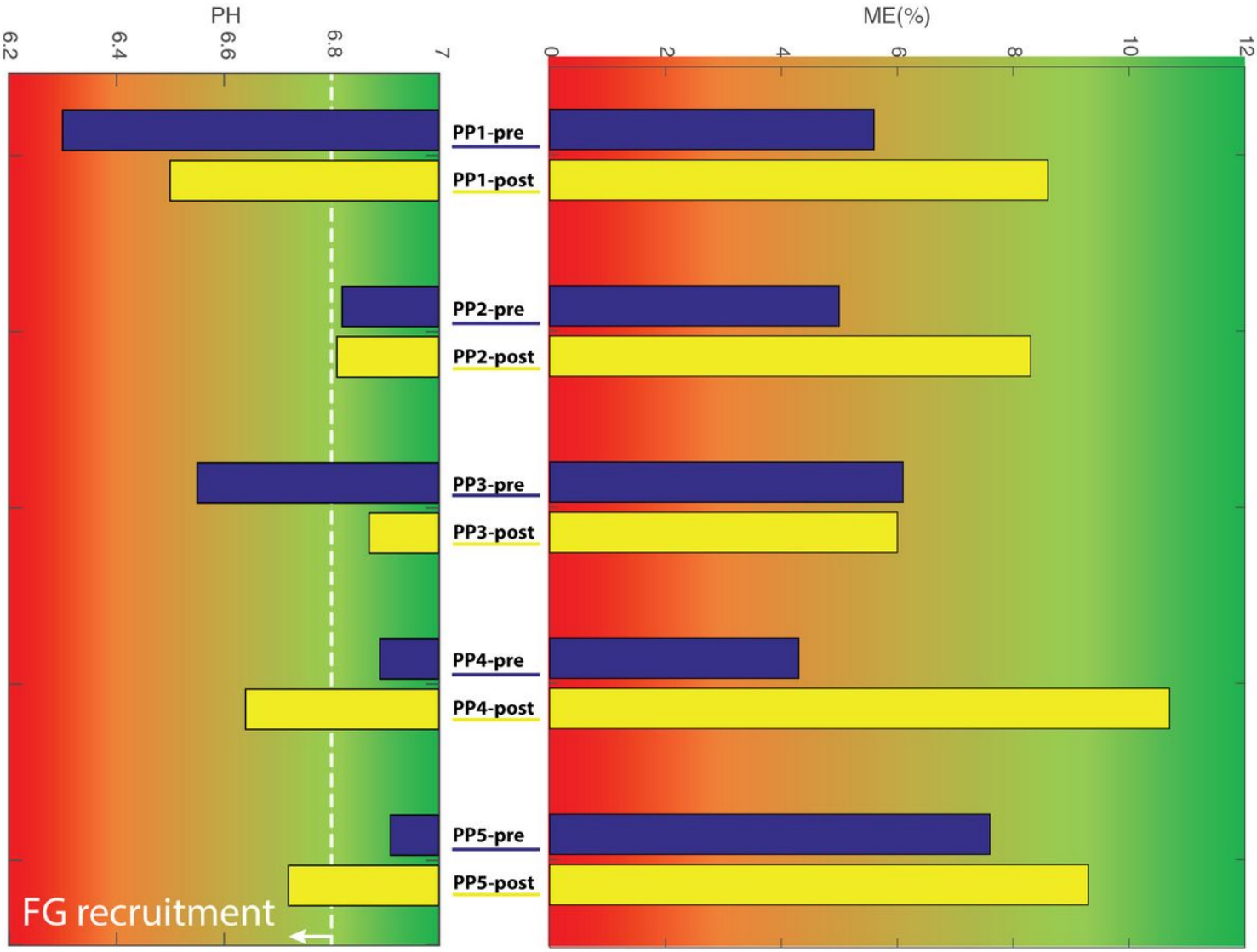

Figure 4

Comparison of magnitude of biceps acidification during ACT (left) versus gross mechanical efficiency (right; %) prior to versus post-training (blue and yellow bars, respectively) for individual subjects.

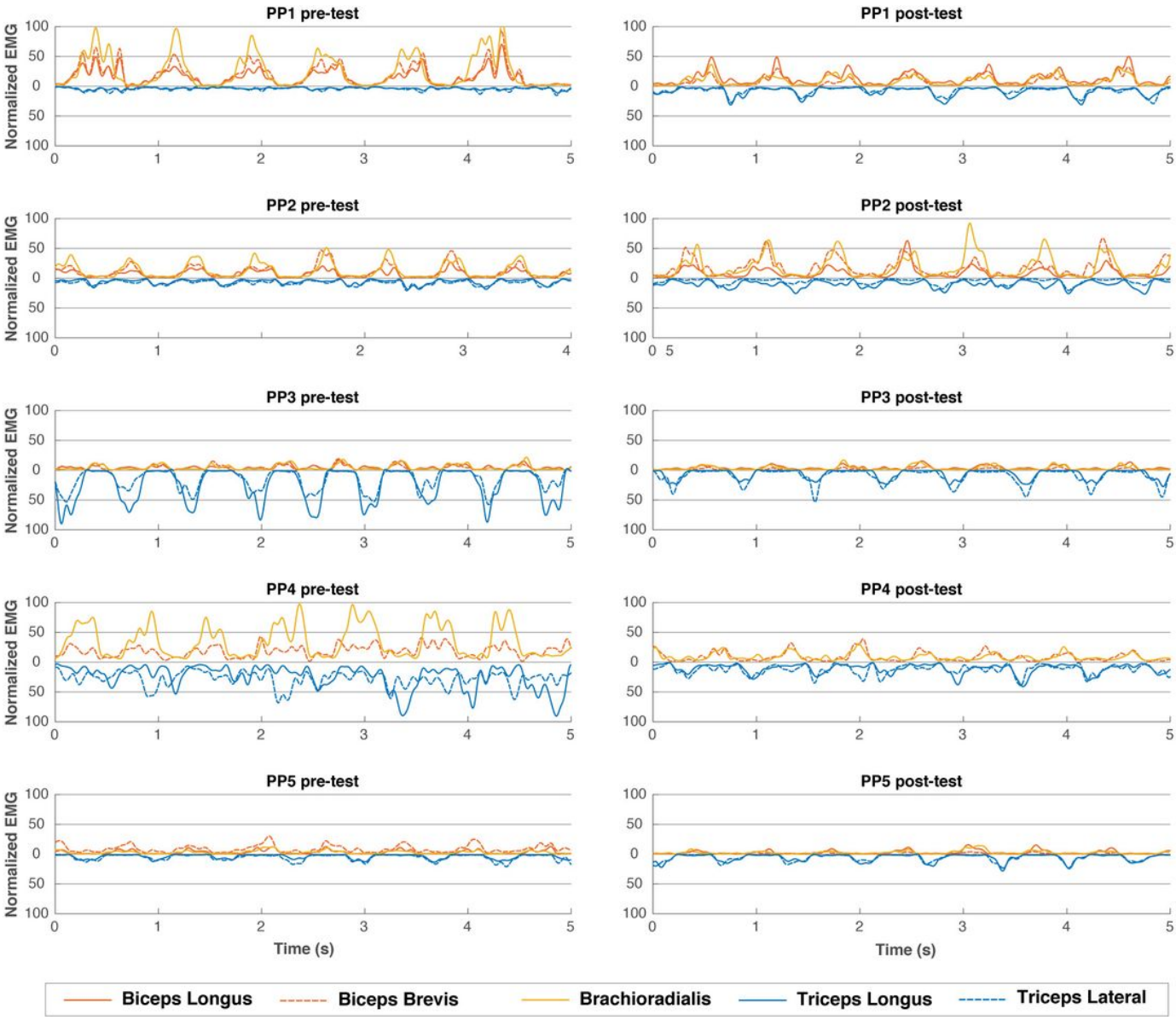

Figure 5

EMG muscle activation pattern over 5 representative seconds during the end of the first minute of the pre- and post-training tests for all individual subjects. Flexor muscles have positive values, extensor muscles are mirrored and depicted as negative values.

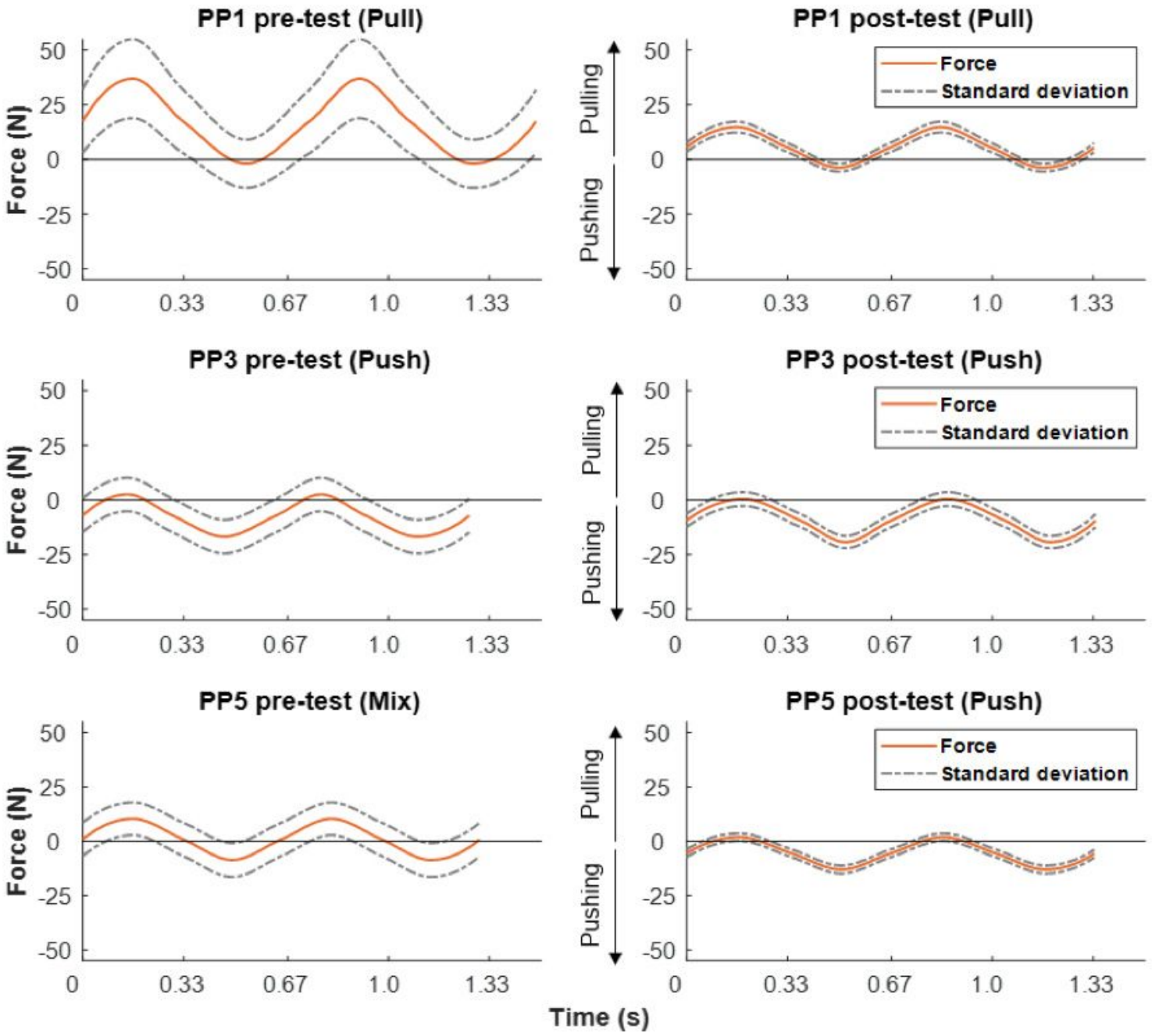

Figure 6

Force output during ACT recorded in pre- (left) versus post-training test (right) in three test-subjects . Positive forces equal pulling and negative forces equal pushing. From top to bottom different individual strategies in terms of pulling, pushing or mixed, respectively, are clearly discernible.

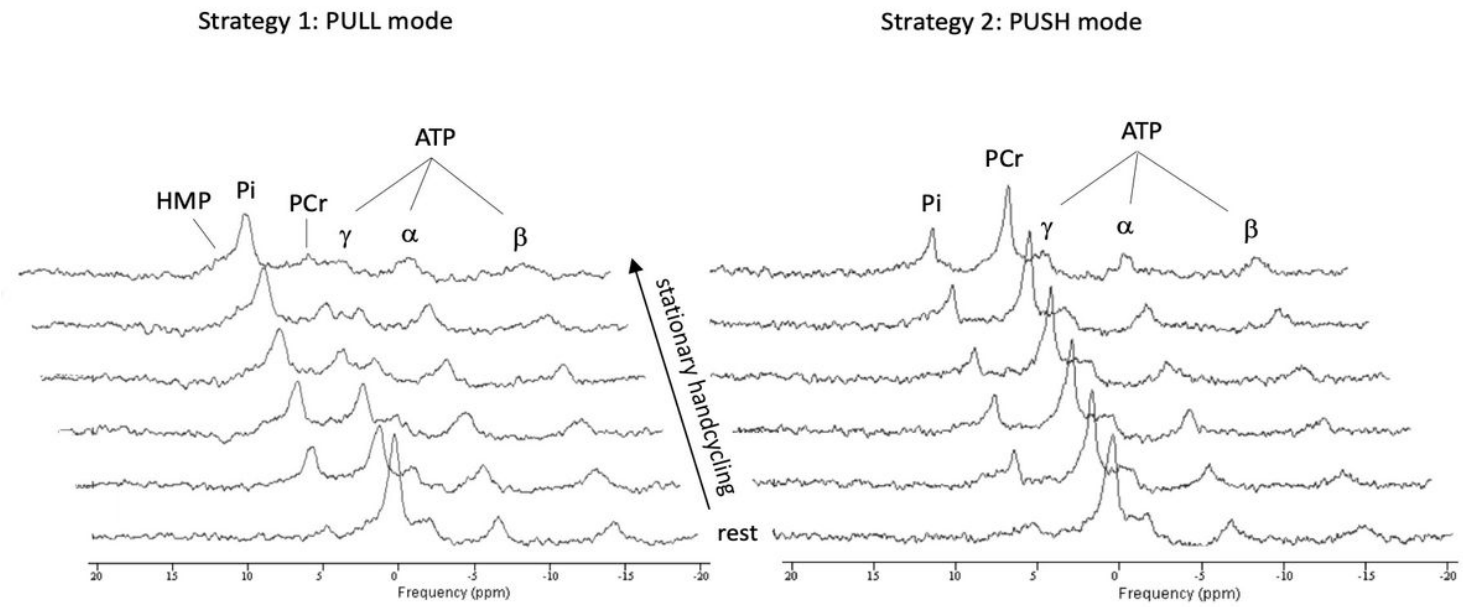

Figure 7

stack plots of in vivo 31P MR spectra recorded from the m. biceps brevis of subjects using either apparent push- (left panel) versus pull- (right panel) arm-cycling strategies, respectively, to generate overall power-output of 15 W required to propel the flywheel at 90 rpm. Each spectrum represents a 11s time-average recording from the biceps muscle. ATP: adenosine triphosphate; Pi: inorganic phosphate; PCr: phosphocreatine; HMP: hexose monophosphate.

Supplementary Files

This is a list of supplementary files associated with this preprint. Click to download.

- SupplementalFigure1.png